J Therm Anal Calorim (2018) 131:2291–2301
https://doi.org/10.1007/s10973-017-6739-9

Hydration mechanism of composite binders containing blast furnace ferronickel slag at different curing temperatures

Jianwei Sun[1] · Zhe Wang[2] · Zhonghui Chen[1]

Received: 10 August 2017 / Accepted: 23 September 2017 / Published online: 6 October 2017

Abstract This study investigated hydration mechanism of composite binders containing blast furnace ferronickel slag at different curing temperatures. Different levels of cement replacement (15, 30, and 45% by mass) and curing temperatures (25 and 60 °C) were set. In addition to pure cement, a composite binder containing quartz with a particle size distribution similar to ferronickel slag was selected as the control sample. The results reveal that blast furnace ferronickel slag can show the pozzolanic reactivity at an early stage at room temperature despite low activity, and an early high curing temperature can improve the activity significantly. The influence of high curing temperature on the pozzolanic reaction is greater than the influence of high curing temperature on cement hydration at an early stage, and as a result, the $Ca(OH)_2$ content in the cementitious system is lowered. However, the influence on the pozzolanic reaction is not obvious in the later stage. The high curing temperature does not change the type of hydration product but increases the content of the C–S–H gel, resulting in a significantly higher Ca–Si ratio and a slightly lower Al–Si ratio. In addition, the high curing temperature improves the early compressive strength of the concrete containing blast furnace ferronickel slag and reduces later compressive strength. A suitable dosage of blast furnace ferronickel slag may improve the resistance to chloride ion penetration of concrete at a high curing temperature.

✉ Jianwei Sun
tbp1600602045@student.cumtb.edu.cn

[1] School of Mechanics and Civil Engineering, China University of Mining and Technology, Beijing 100083, China

[2] School of Chemical and Environmental Engineering, China University of Mining and Technology, Beijing 100083, China

Keywords Ferronickel slag · Hydration · Compressive strength · Permeability

Introduction

Currently, concrete has been used as the principal construction material in the world, which results in a large amount of cement produced and consumed [1]. Despite the extraordinary and notable progress over the past decade, the production of 1 ton of cement generates average CO_2 emissions ranging from 0.60 to 1 ton, which depends on the cement type and production process [2]. Therefore, to reduce the cement production in the concrete stage, supplementary cementitious materials (SCMs) are being widely used as alternative materials for the partial or total replacement of cement [3].

The most common SCMs are pozzolanic materials, including natural pozzolans (zeolite, metakaolin), by-products (fly ash, silica fume), and metallurgical slags (blast furnace slag, manganese slag) [4]. The hydration of cement–SCM binders includes two interrelated processes: the hydration of cement clinker and the pozzolanic reaction of SCM. $Ca(OH)_2$ (CH) is produced during the hydration of cement clinker and consumed by the pozzolanic reaction of SCM. In addition to the pozzolanic reaction, the addition of SCM decreases the amount of cement required and increases the effective water-to-cement ratio. Besides, the fine particles of SCM can act as heterogeneous nucleation sites on which the hydration products could precipitate. Moreover, the filling effect of SCM can make the paste matrix and the interfacial transition zone between matrix and aggregate denser [5, 6]. Adding pozzolanic admixtures is an effective way to lower hydration heat, improve workability, perfect porous microstructure, reduce cracks,

and enhance resistance to chlorides, sulfates, and fire, as well as mitigate the alkali–silica reaction [7, 8]. In addition, many SCMs used would reduce the land use owing to stacking and landfill as well as avoid pollution to air or groundwater due to dust or heavy metals. Blast furnace slag from pig iron production and fly ash from coal combustion are the most popular choices as SCMs, and these materials have been extensively studied over the past decades. However, with the shortage in supply and rise in price of slag and fly ash, it is worthwhile to develop other potential SCMs for concrete [9].

Ferronickel slag, an industrial waste obtained from smelting of laterite, garnierite, or pentlandite ores at a high temperature in the presence of a reducing agent, is cooled with water or air [10, 11]. The percentage of ferronickel slag generated in the processing of nickel ore can reach 50–75%, and almost 14 tons of ferronickel slag is generated per ton of ferronickel production [12, 13]. A large amount of ferronickel slag is produced worldwide, and the annual output is more than 4 million tons in China [14]. However, less than 10% of ferronickel slag is utilized, and it is essential to find feasible and viable applications of the ferronickel slag that can ensure its maximal utilization [15]. Due to the differences between the raw ore and the smelting process, the chemical compositions of ferronickel slags are different significantly. Safe disposal and application of the slag is considered as a major issue worldwide. One of the biggest concerns in using ferronickel slag is the relatively high chromium content. This metal is found as a trivalent chromium. However, the Cr^{3+} contained mainly in the spinel phase is stable and is not soluble in water when ferronickel slag is used as a mineral admixture, not expected to be leached out during the hydration process [16]. The soundness of ferronickel slag due to divalent magnesium is another concern. However, Muhammad et al. used high-magnesium ferronickel slag to find no increase in expansion using up to 65% ferronickel slag. Mg^{2+} was found to be in the form of stable forsterite ferroan that did not take part in the hydration, and expansive $Mg(OH)_2$ (brucite) was not found in the microstructure [17].

Two types of ferronickel slag are produced depending on the production process, including electric furnace slag and blast furnace slag. Electric furnace ferronickel slag has been studied extensively abroad for the past few decades. Among the several previous studies reported, the most important aspects are related to: (1) the construction of roads, to replace the coarse aggregates in the production of subbase materials and anti-slip blacktop [16], (2) the production of cement and concrete, as additives in the Portland cement or as a substitute for natural aggregates [16, 18, 19], and (3) the production of building materials, as additives in ceramic tiles and bricks, in fire-resistant bricks, and in anti-slippery pavement tiles [20, 21].

The reactivity of blast furnace ferronickel slag (BF) is higher due to a greater glassy-phase content, which is more suitable as SCM than electric furnace ferronickel slag. However, there are relatively few studies on the BF used as the mineral admixture. Meanwhile, the temperature inside massive concrete structures and even concrete members with high casting temperature is significantly higher than the standard curing temperature in the laboratory. The chemical reaction rate is significantly affected by temperature according to Arrhenius law [22]. Most of the results also found in the literature that the curing temperature affects hydration of the composite binders and structure of the hardened pastes. To a certain extent, the reaction degree of the composite binder increases with elevated curing temperature [23]. The accelerated hydration can produce more C–S–H gel, increase the density of the matrix, and result in superior mechanical properties of concrete at an early stage. The later compressive strength of the concrete under the higher-temperature curing condition is typically lower [24, 25]. Many studies also showed that the reactivity of SCMs was found to be more sensitive to temperature than the hydration of Portland cement [22, 23, 25–27].

Therefore, the influence of elevated curing temperature on the hydration of composite binders containing BF deserves further investigation. Furthermore, the corresponding performance of the concrete should be discussed for engineering application.

Experimental

Raw materials

Cement with the grade of P.I 42.5 complying with Chinese National Standard GB 175 (equivalent to European CEM I 42.5) was utilized in this study. The other raw materials used in this study included BF and inert quartz powder (QZ). The chemical oxide composition of each powder is presented in Table 1. The oxide composition was obtained by X-ray fluorescence (XRF) spectroscopic analysis. Compared with those in cement, the SiO_2 content and Al_2O_3 content in BF are obviously higher, but the CaO content is lower. The MgO content of BF used is 12.54%. The chemical composition of QZ as an inert admixture is almost SiO_2.

The X-ray diffraction (XRD) pattern of BF (presented in Fig. 1) reveals its amorphous nature, as reflected by the presence of a diffuse wide band from the glassy phase. The complex spinel phase [$(Fe^{2+}, Mg)(Fe^{3+}, Al, Cr)_2O_4$] and $CaCO_3$ crystals were the main crystalline mineralogical phase that was detected in the slag. The formation of crystalline phases is a combined action between the

Table 1 Chemical compositions of raw materials/%

Composition	CaO	SiO_2	Fe_2O_3	Al_2O_3	MgO	MnO	Cr_2O_3	SO_3	Na_2O	K_2O
Cement	61.20	22.16	4.89	4.18	3.26	0.09	0.04	2.72	0.09	1.23
BF	22.50	33.15	2.15	21.94	12.54	2.36	2.08	1.31	0.32	0.36
QZ	0.01	99.76	0.01	0.04	0.01	–	–	–	–	0.01

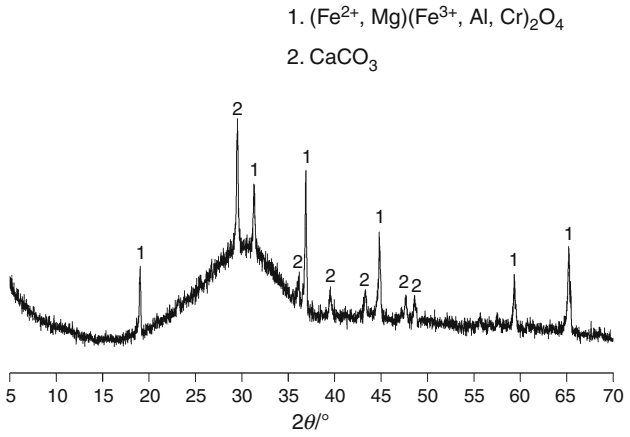

Fig. 1 XRD analysis of BF used

chemical composition of the melt and its cooling rate. In the case of a high content of silica, the slag vitrifies (forms a glassy phase) under rapid cooling. There is no periclase phase despite the high content of MgO in BF, which is consistent with previous research results [16, 17].

The particle size distribution of each powder, determined using a laser particle size analyzer (Mastersizer 2000), is shown in Fig. 2. Figure 2 shows that the distribution of BF and QZ is close to the distribution of cement.

The fine aggregate consisted of river sand with a specific gravity of 2.65 and a fineness modulus of 2.59. The crushed limestone as coarse aggregate consisted of 25 mm maximum size basalt with a specific gravity of 2.65. All aggregates conforming to Chinese Standard JGJ 52-2006 were prepared. Polycarboxylate-based superplasticizer was used to adjust the workability of the mixtures.

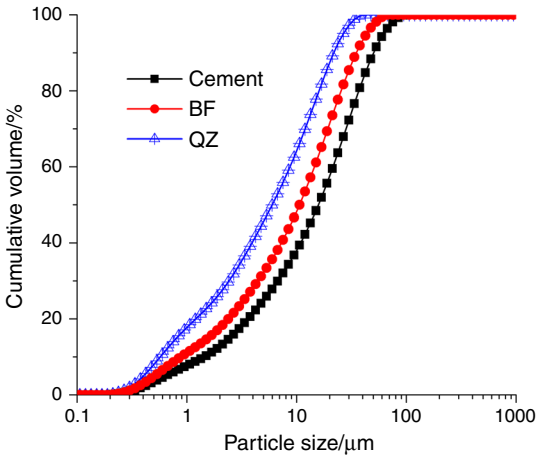

Fig. 2 Particle size distribution of raw materials

Mix proportions

The mix proportions chosen for this study are given in Table 2. Seven different concrete mixtures with a water/binder ratio of 0.4 were prepared, but the compositions of the binders were different. A pure cement sample (sample C) was used as the reference sample. Three replacement ratios (15, 30, and 45% by mass) of BF and QZ were chosen.

Test methods

The exothermic rate and the cumulative hydration heat of the binders were measured at constant temperatures of 25 and 60 °C with an isothermal calorimeter (TONI7338). TONI7338 has eight parallel twin-chamber measuring channels; one chamber contains the sample, and another contains the reference. To avoid considerable temperature difference between the paste and the isothermal environment, binder and water were kept at a temperature close to the measurement temperature before mixing. The pastes were immediately placed into the chamber after mixing.

To examine the hydration products, the pastes were cast into plastic centrifuge tubes. Then, the pastes were left to cure at 25 °C (symbol S) and 60 °C (symbol H) in temperature-controlled sealed vessels containing tap water. At

Table 2 Mix proportions of concretes/kg m^{-3}

Sample	Cement	BF	QZ	Sand	Stone	Water
C	420	0	0	769	1063	168
BF-15	357	63	0	769	1063	168
BF-30	294	126	0	769	1063	168
BF-45	231	189	0	769	1063	168
QZ-15	357	0	63	769	1063	168
QZ-30	294	0	126	769	1063	168
QZ-45	231	0	189	769	1063	168

certain stages, the hardened pastes were cut into pieces and put into absolute alcohol to extract the free water for 1 day and then dried in the oven at 80 °C to a constant mass. The non-evaporable water contents of the hardened pastes were tested at 3, 28, and 90 days by calculating the mass loss of samples between 80 and 1060 °C. The loss on ignition of raw material has been considered during the calculation of the mass loss. The CH content of the paste was calculated based on the TG/DTG curve. The TG/DTG curve was obtained at 28 and 90 days after grinding by using a thermogravimetric analyzer (NETZSCH STA 449F3) with a heating rate of 10 °C min^{-1} from 30 to 900 °C in a nitrogen atmosphere. XRD analysis was performed with a scanning range from 5° to 70° (2θ) and a measuring speed of 8° min^{-1}. The morphologies of the hardened pastes were observed with scanning electron microscopy (SEM) using an FEI Quanta 200 instrument. The chemical compositions of the hydration products were measured by energy dispersive X-ray (EDX) analysis.

Concrete cubes of 100 × 100 × 100 mm were prepared. After casting, some specimens were placed in a standard curing room with a constant temperature and humidity (20 ± 1 °C, 95% RH). The other specimens were placed in a steam curing chamber with a constant temperature of 60 °C for the initial 7 days and then cured in the standard curing room to the certain stages. After curing, the compressive strengths of the concretes were determined according to the Chinese National Standard GB/T 50081-2002. Tests of strength were performed at the age of 3, 28, and 90 days after casting by using three specimens for each test. With the same curing method as the compressive strength, the permeability of the concrete to chloride ion was tested at the age of 28 and 90 days according to ASTM C1202 "Standard Test Method for Electrical Indication of Concretes Ability to Resist Chloride Ion Penetration".

Results and discussion

Hydration heat

In general, the hydration process of cement-based material can be divided into five stages: the rapid exothermic stage, the dormant stage with low exothermic rate, the hydration accelerating stage, the hydration decelerating stage, and the steady stage. The acceleration period corresponds mainly to the C_3S hydration and generation of C–S–H gel and CH crystal. The exothermic rate of the composite binder depends on three main factors: the cement content, the activity of the mineral admixture, and the effect of adding the admixture on cement hydration [7, 8, 28]. QZ is a totally inert admixture in the cementitious system. However, the addition of QZ decreases the amount of cement and increases the effective water-to-cement ratio, and the fine particles of QZ can enhance heterogeneous nucleation of C–S–H gel. Thus, QZ can promote the early hydration of cement. In addition, the filling effect of QZ can make the paste matrix and the interfacial transition zone between aggregates and cement matrix denser. BF not only has physical effects similar to those of QZ but also has pozzolanic activity and can react with CH to form C–S–H.

The exothermic rate and the cumulative hydration heat per unit mass of the binders at 25 °C are shown in Fig. 3a, b, respectively. Figure 3a shows that replacing a high amount of cement by mineral admixture tends to advance the second exothermal peaks (after the hydration accelerating stage) and lower peak values. The former is owing to the increased nucleation sites provided by fine QZ or BF,

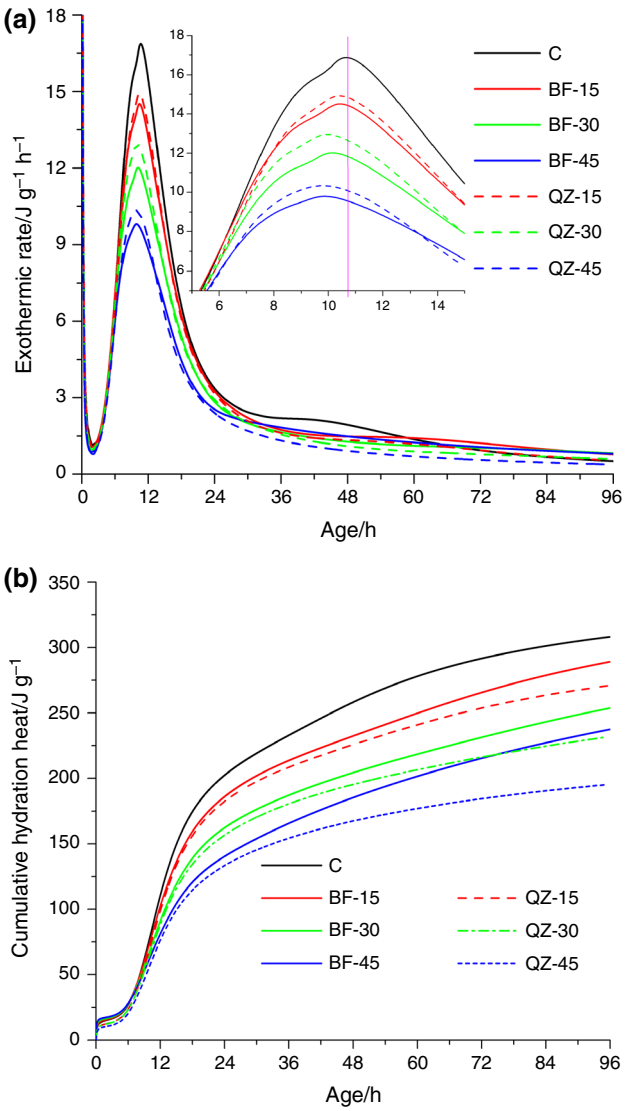

Fig. 3 Exothermic rate and the cumulative hydration heat of binders at 25 °C. **a** Exothermal rate. **b** Cumulative hydration heat

and the latter is due to the reduction in cement content. The exothermal peaks of composite binders containing QZ are slightly higher than those containing BF due to the finer particles of QZ. In the decelerating stage, with the same cement replacement, the exothermic rates of composite binders containing BF or QZ are very close. However, in the late deceleration, the exothermic rates of composite binders containing BF gradually exceed the exothermic rates of composite binders containing QZ, even more than the exothermic rates of the pure cement after 60 h, indicating that the pozzolanic reaction of BF is obviously promoted. The cumulative hydration heats of samples C, BF-15, BF-30, and BF-45 at 25 °C after the steady stage are 308, 288, 253, and 238 J g^{-1}, respectively. The cumulative hydration heats of samples QZ-15, QZ-30, and QZ-45 are 270, 233, and 196 J g^{-1}, respectively. The cumulative hydration heats decrease with the addition of mineral admixture due to the reduction in cement content. Even though the pozzolanic reaction of BF is promoted after 60 h, it cannot compensate for the reduced heat due to the decrease in cement content. At the same dosage, the cumulative heats of the samples containing BF are higher than those of the samples containing QZ. The increments of hydration heats from the samples containing QZ to the samples containing BF at 15, 30, and 45% replacement levels are 18, 20, and 42 J g^{-1}, respectively. The result shows that BF can participate in the reaction at an early stage at 25 °C.

The exothermic rate and the cumulative hydration heat per unit mass of the binders at 60 °C are shown in Fig. 4a, b, respectively. The exothermal peaks occur in advance, which shows that high temperature promotes the hydration degree of each binder. It is 6 h at 60 °C as compared to 60 h at 25 °C that the exothermic rates of composite binders containing BF exceed the exothermic rates of the pure cement, indicating that the reactivity of BF is activated by the high temperature. The cumulative hydration heats of samples C, BF-15, BF-30, and BF-45 after the steady stage are 336, 338, 342, and 322 J g^{-1} at 60 °C, respectively, which are increased by 9, 17, 35, and 35%, respectively, compared to the results at 25 °C. The cumulative hydration heats of samples QZ-15, QZ-30, and QZ-45 are 304, 255, and 200 J g^{-1}, respectively, which are increased by 13, 9, and 2%, respectively. The growth rates of the hydration heats of binders containing BF are more than those of binders containing QZ, and furthermore, the cumulative heats of BF-15 and BF-30 are more than those of C, which states clearly that the effect of high curing temperature on the pozzolanic reaction is greater than the effect of high curing temperature on cement hydration. Nevertheless, the cumulative heat of BF-45 is less than the cumulative heat of pure cement, because the heat decrement with the sharp decrease in the amount of cement is higher than the heat

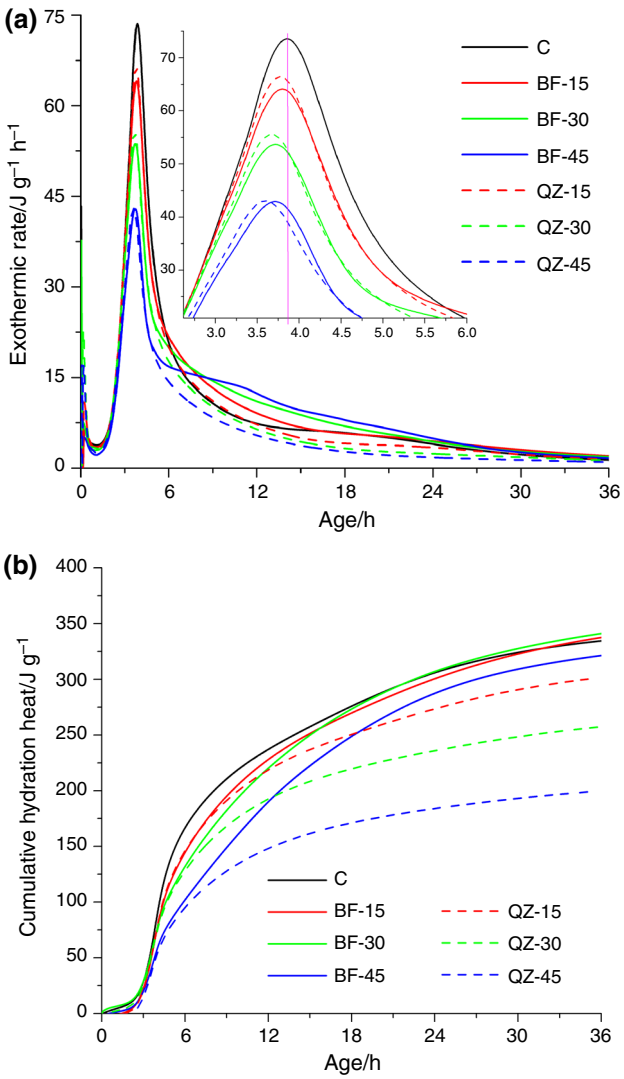

Fig. 4 Exothermic rate and the cumulative hydration heat of binders at 60 °C. **a** Exothermal rate. **b** Cumulative hydration heat

increment generated due to the influence of high curing temperature on the pozzolanic reaction.

Non-evaporable water content

For the hardened pastes with the same kinds of hydration products, the non-evaporable water content represents the amount of hydration products and is the important index of the hydration degree. The non-evaporable water content of the pastes at 3, 28, and 90 days under two different curing conditions is displayed in Table 3. The non-evaporable water content increases with the prolongation of the age with the enhancement of the hydration degree. As expected, the non-evaporable water contents of the pastes containing BF and QZ are smaller than those of the pure cement paste under all curing ages at 25 °C, due to the reduction in the cement content. The non-evaporable water

Table 3 Non-evaporable water content of the hardened paste/%

Sample	3 days		Increasing rate	28 days		Increasing rate	90 days		Increasing rate
	25/°C	60/°C		25/°C	60/°C		25/°C	60/°C	
C	12.70	15.62	23.0	17.25	17.70	2.6	18.25	18.38	0.7
BF-15	12.04	15.56	29.2	16.41	17.73	8.0	17.70	18.64	5.3
BF-30	11.43	15.43	35.0	15.59	17.16	10.1	17.40	18.23	4.8
BF-45	10.61	14.98	41.2	15.10	16.34	8.2	17.24	17.97	4.2
QZ-15	11.59	14.07	21.4	15.01	15.47	3.1	16.74	16.84	0.6
QZ-30	10.54	12.64	19.9	13.76	14.06	2.2	14.80	14.93	0.9
QZ-45	9.33	10.76	15.3	10.63	11.14	4.8	11.69	11.76	0.6

contents of the pastes containing BF are higher than those of the pastes containing QZ, primarily due to the pozzolanic reaction of BF, which produces more extra C–S–H gel. The increments are significantly larger at 90 days. It is an indication that the pozzolanic reaction of BF is promoted at a later stage.

All the growth rates of the non-evaporable water contents at 3 days at 60 °C were above 15%, which indicates that the hydration degree of each binder of cement hydration and pozzolanic reaction is stimulated by the initial high curing temperature. However, the improvement in high temperature in the non-evaporable water contents at 28 and 90 days is much smaller, possibly because the rapid hydration of cement in an early stage under high curing temperature tends to produce many hydration products, which form a thick dense gel layer around the unhydrated particles [22, 25]. The increments of the non-evaporable water contents of the pastes containing BF are higher than the increments of the pure cement and composite binders containing QZ. The non-evaporable water content of BF-15 is greater than that of the pure cement after 28 and 90 days, indicating that the high curing temperature activates the reactivity of BF and the reaction of BF makes a considerable contribution to the further growth of the non-evaporable water content.

CH content

The TG/DTG curves of the hardened pastes (C, BF-30, and QZ-30) at 28 and 90 days are presented in Figs. 5 and 6, respectively. Two common endothermic peaks are observed on the DTG curves of all samples, corresponding to the partial dehydration of C–S–H and ettringite (below 200 °C) and the decomposition of CH (at approximately 400–500 °C), respectively. Another endothermic peak can be observed on the DTG curves of certain samples at approximately 600–800 °C corresponding to the

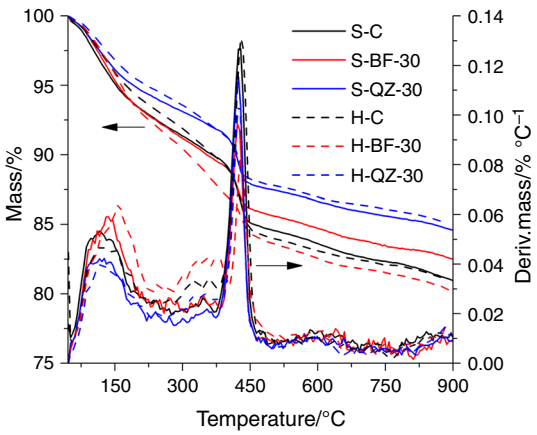

Fig. 5 TG/DTG curves of the hardened pastes at 28 days

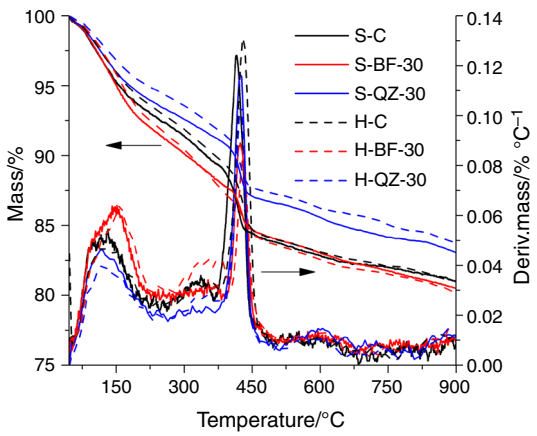

Fig. 6 TG/DTG curves of the hardened pastes at 90 days

decomposition of $CaCO_3$, which is formed due to the carbonization reaction of CH or from BF.

Flaky CH crystal is a weak part in the hardened pastes. High content of CH tends to cause a negative effect on the microstructure of paste. CH crystal is formed by the hydration of cement and consumed by the pozzolanic

reaction of BF. Therefore, the CH content plays a dominant role in the interaction between the hydration of cement and the pozzolanic reaction of BF. The content of CH in the pastes is calculated according to the data of TG. Figure 7 shows the CH contents of all samples cured at both 25 and 60 °C. As expected, the CH content of the samples containing BF or QZ is smaller than those of the pure cement due to the decrease in the cement content. The CH content of BF-30 is obviously smaller than the CH content of QZ-30 because of the consumption by the pozzolanic reaction of BF.

The CH contents of the pure cement are also normalized with the corresponding coefficient of 0.7 for comparison with the CH content of the pastes containing 30% BF and QZ to demonstrate the effect of BF and QZ more clearly. The CH contents of the pastes containing QZ are evidently significantly higher than the CH contents of the pure cement paste after normalization by the adjustment coefficient under different curing condition. This upsurge in the amount of CH produced is attributed to the positive influence of the physical effect of QZ on the hydration of cement.

The CH content from the physical effect of QZ (W_1) can be calculated by Eq. (1). Here, W_{QZ} is the CH content of the composite binder containing QZ, and $W_{0.7C}$ is the CH content of the pure cement after normalization by the adjustment coefficient of 0.7.

$$W_1 = W_{QZ} - W_{0.7C} \quad (1)$$

Consequently, the increments in CH contents due to the physical effect of QZ after curing for 28 and 90 days at 25 °C are 2.11 and 2.22%, respectively. And those are 1.94 and 2.07%, respectively, at 60 °C. The increments from 28 days to 90 days increase because of the higher hydration degree of cement with the prolongation of the aging period. In addition, the increments at 60 °C are less than the increments at 25 °C, possibly because the hydration product layer after the high temperature is denser, resulting in QZ having little effect on cement hydration, which is in agreement with the results of the non-evaporable water contents.

Similarly, the CH consumption owing to the pozzolanic reaction of BF (W_2) can be calculated by Eq. (2). Here, W_{BF} is the CH content of composite binder containing BF.

$$W_2 = W_{QZ} - W_{BF} \quad (2)$$

Hence, the consumptions of CH due to the pozzolanic reaction of BF after curing for 28 and 90 days at 25 °C are 1.44 and 4.38%, respectively. The values are 4.1 and 5.9% at 60 °C. From 28 to 90 days, the reaction degree of the pozzolanic reaction improves 204 and 44% at 25 and 60 °C, respectively. The result shows that the CH content of the pastes containing BF is larger than the CH content of the pure cement paste after normalization by the adjustment coefficient after curing for 28 days at 25 °C, which indicates that the amount of CH is greater than its consumption. In other words, the physical effect of BF on cement hydration is stronger than the pozzolanic reaction. However, with the prolongation of the aging period, the pozzolanic reaction consumes a large amount of CH, so that the reaction degree increases more than 200%. Compared to the phenomenon at 25 °C, it appears opposite at 60 °C, which indicates that the pozzolanic reaction of BF has consumed some CH. The change in reaction degree is unobvious.

High curing temperature brings about the increasing reaction degree of BF at 28 and 90 days of 185 and 35%, respectively. It is also an indication that high temperature promotes the pozzolanic reaction of BF.

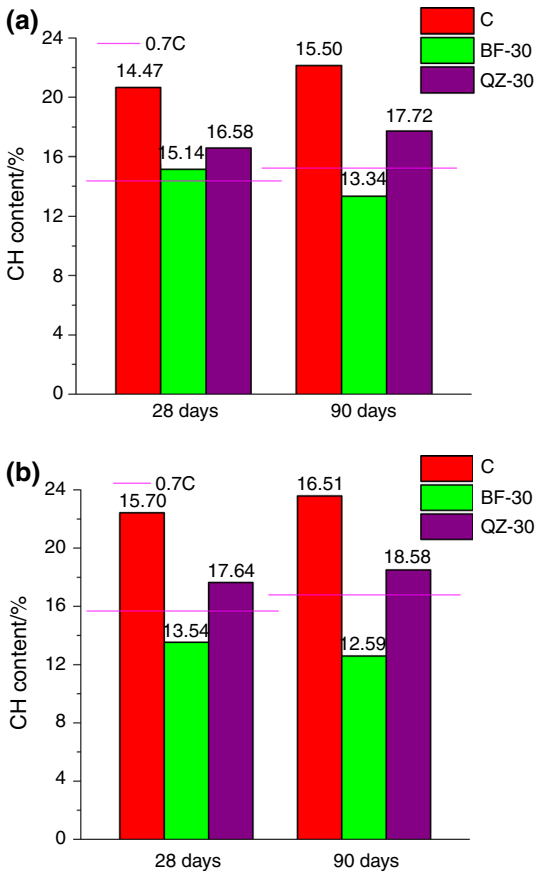

Fig. 7 The CH content of the hardened paste at 90 days. **a** 25 °C. **b** 60 °C

XRD and SEM analysis

Figure 8 shows the XRD patterns of BF-30 at 90 days under two curing temperatures. As shown in Fig. 8, no clear observed difference exists between specimens. The hydration products mainly include CH and AFm in addition to C_2S, C_3S, and C_4AF from unhydrated cement

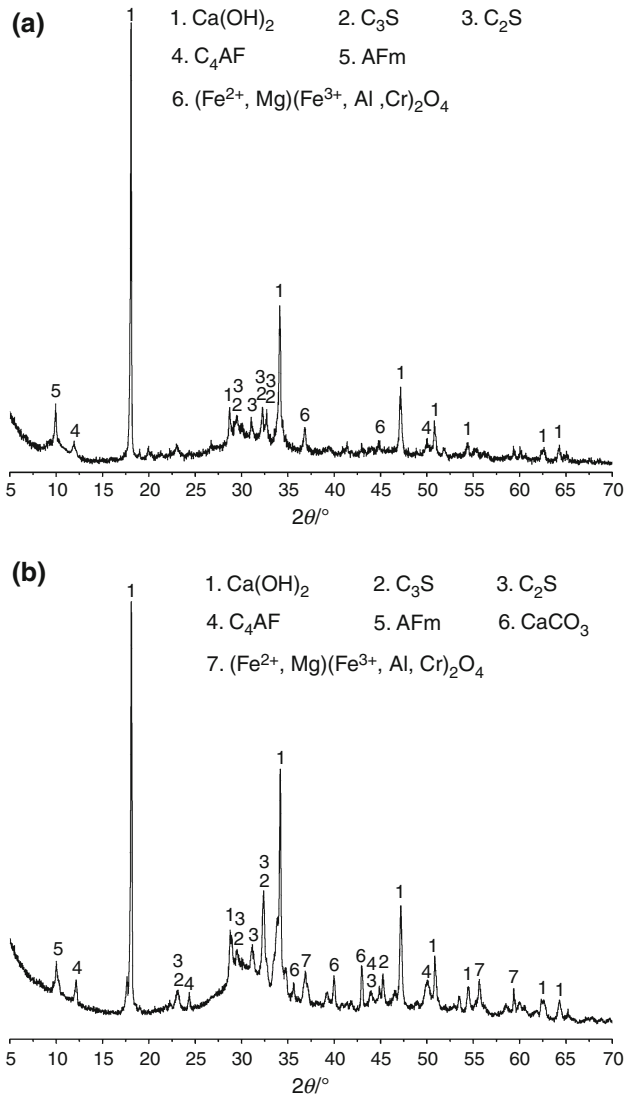

Fig. 8 XRD patterns of BF-30 at 90 days. **a** 25 °C. **b** 60 °C

clinkers as well as $(Fe^{2+}, Mg)(Fe^{3+}, Al, Cr)_2O_4$ and $CaCO_3$ from unreacted BF. Therefore, high curing temperature does not bring new crystalline minerals.

Figures 9 and 10 show SEM images of BF-30 at 90 days under two curing temperatures. In contrast to BF-30 cured at 25 °C (Fig. 9), the microstructure of BF-30 cured is denser at 60 °C (Fig. 10), which indicates that the high temperature promotes the pozzolanic reaction of BF, improving the inner structure and the microcosmic physical properties. The hydration products are covered by the amorphous gel, which is C–S–H gel determined by EDX analysis. Moreover, massive particles coated by C–S–H gels are mainly spinel crystals. Therefore, spinel is relatively stable at high temperature and does not react.

The mole fractions of elements of C–S–H gel were calculated based on EDX analysis. For each sample, 80 microareas of C–S–H gel were tested. Figure 11 shows the

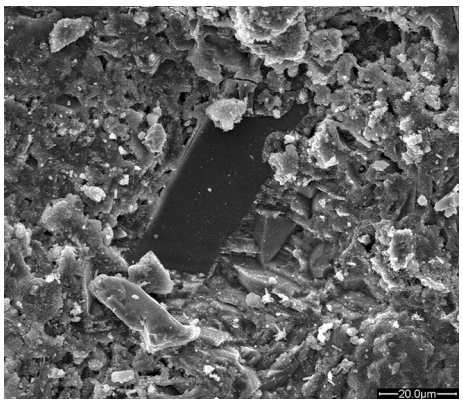

Fig. 9 SEM image of BF-30 at 25 °C

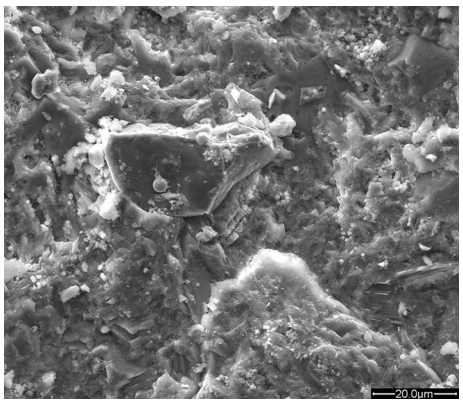

Fig. 10 SEM image of BF-30 at 60 °C

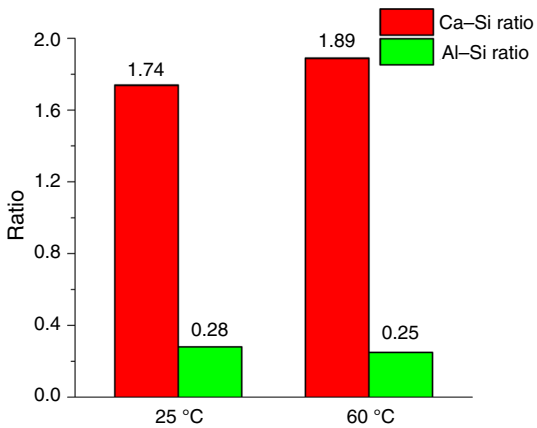

Fig. 11 Ca–Si ratios and Al–Si ratios of the C–S–H gel

mean Ca–Si and Al–Si ratios of C–S–H gel from BF-30. Figure 11 shows that the mean Ca–Si ratios of the C–S–H gel from BF-30 at 25 and 60 °C are 1.74 and 1.89, respectively. The difference in the Ca–Si ratio of C–S–H gel is significant. The mean Ca–Si ratio becomes higher. Although the calcium content in BF is significantly lower

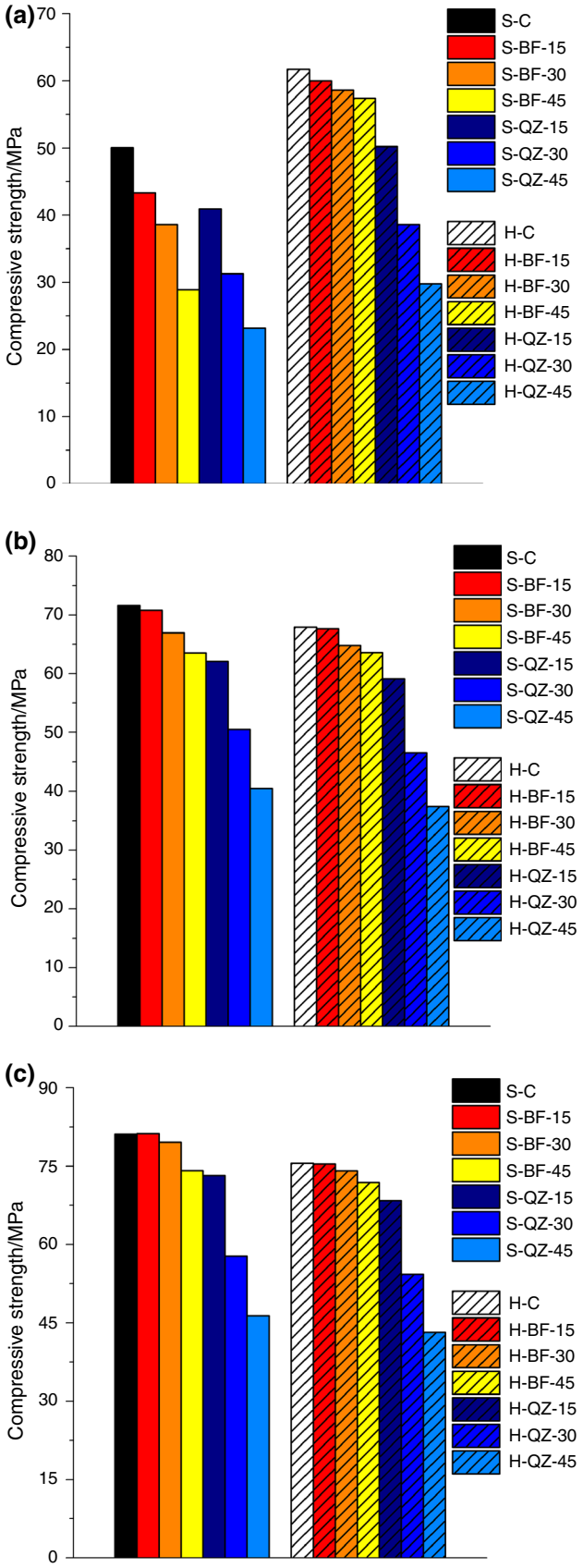

◀**Fig. 12** Compressive strengths of the concrete. **a** 3 days. **b** 28 days. **c** 90 days

than the calcium content of the cement, the cement content in the composite binder accounts for 70%, and the contribution of cement hydration is greater than the contribution of BF at high curing temperature at 90 days.

Figure 11 shows that the mean Al–Si ratios of the C–S–H gel from BF-30 at 25 and 60 °C are 0.28 and 0.25, respectively. The results show that the mean Al–Si ratio is slightly lower under normal temperatures. Table 1 shows that the content of aluminum in BF is much higher than the content of aluminum in the cement, and the aluminum content in the composite binder is very high. Although the high curing temperature improves the reaction degree of the composite binder, it has little effect on the Al–Si ratio.

Compressive strength of concrete

Figure 12 shows the compressive strengths of all specimens with a water/binder ratio of 0.4 at the ages of 3, 28, and 90 days. As expected, the compressive strengths of the concretes containing the mineral admixture are smaller than the compressive strengths of the pure cement concrete after curing 3 days at 25 °C due to the reduction in cement content. However, the compressive strengths of the concretes containing BF are higher than the compressive strengths of the concretes containing QZ after curing 3 days, which illustrates that the pozzolanic reaction of BF occurs at an early stage. Apparently, the compressive strengths of all samples subjected to high temperature increase. The strength growth rate of sample C is 23.4%. The strength growth rates of samples BF-15, BF-30, and BF-45 are 38.6, 51.8, and 98.6%, respectively. The strength growth rates of samples QZ-15, QZ-30, and QZ-45 are 22.7, 23.3, and 28.4%, respectively. The strength growth rate of the pure cement concrete is the lowest, indicating that the influence of increasing curing temperature on the early strength of concrete with mineral admixture is more significant [29]. In general, the result of the compressive strength determinations at 3 days is consistent with the results of hydration heat and the non-evaporable water contents.

However, the compressive strength of all samples at 28 and 90 days is reduced when they are subjected to high temperature. Some studies found that high early-age curing temperature has the negative effect on the late-age mechanical properties [25, 30]. On the one hand, the elevated-temperature curing at early age promotes the hydration of cement and produces a dense C–S–H gel layer. A dense gel layer may hinder the late reaction. On

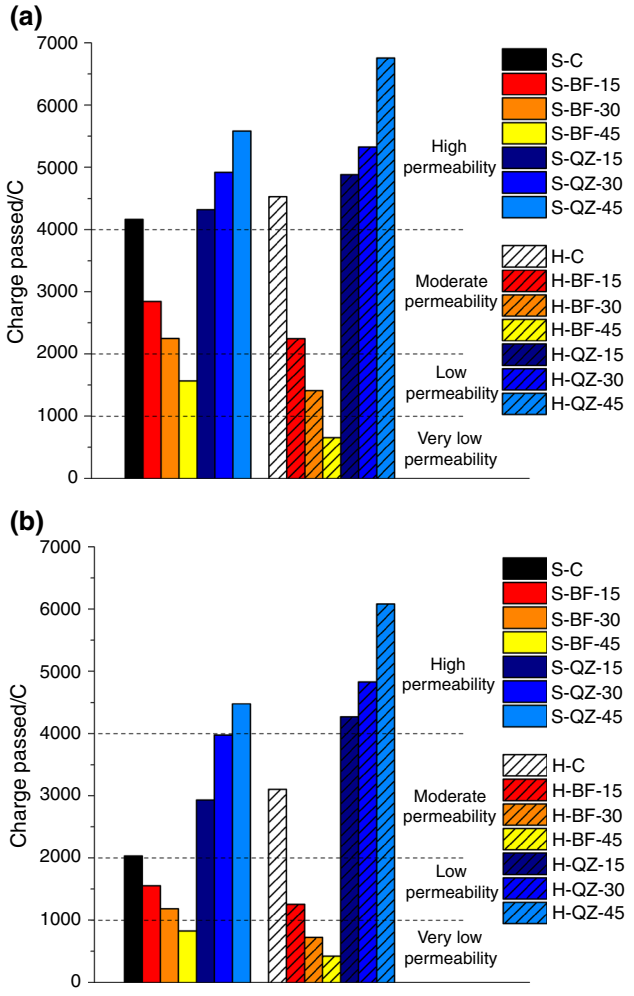

Fig. 13 Chloride permeability of concrete. **a** 28 days. **b** 90 days

the other hand, the elevated-temperature curing at early age makes the hydration products distribute non-uniformly, forms large pores, and increases in cumulative pore volume, which influences the mechanical properties of concrete. Therefore, although the pozzolanic reaction of BF has a positive effect on the later strength, it could not compensate for the adverse effect of early high temperature on the later strength.

The compressive strengths of the pure cement concretes and concretes containing BF at 28 and 90 days under the same curing conditions vary insignificantly. It is an indication that the pozzolanic reaction of BF plays a more dominant role in the increase in compressive strength of concretes at the later stage than physical effects, which corresponds to the result of thermogravimetric analysis.

Chloride ion penetration in concrete

Chloride ion penetration in concrete is closely related to the porosity and connectivity of the pores of concrete. Figure 13 shows the charge passed and permeability grades of the concrete at 28 and 90 days according to ASTM C1202.

Apparently, incorporation of BF decreased the permeability of concrete under standard curing conditions. With the growth of cement replacement, the decreasing extent was larger. Figure 13 shows that the permeability of the concrete containing 45% BF (sample S-BF-45) falls in the "Low" level at 28 days and falls in the "Very Low" level at 90 days, which improves two grades compared to the pure cement concrete. Nevertheless, the effect of QZ is opposite to the effect of BF. It is evident that the charge passed increases with the increase in QZ content. The permeability of all concrete containing QZ falls in the "High" level at 28 days, and sample S-QZ-45 still falls in the "High" level at 90 days. It is an indication that the permeability of all concrete is not improved only by the physical effects of mineral admixture, and the pozzolanic effect of BF is the main contribution to the late-age penetration by reducing connectivity of pores.

Compared with curing at standard conditions, the charge passed in concrete containing QZ and pure cement concrete under steam curing condition increases, regardless of ages. For concrete containing QZ, although the charge passed decreases with the increase in ages, the chloride permeability grade is still "High," not changed. This result indicates that the elevated-temperature curing at early ages has a disadvantageous influence on the resistance to chloride ion penetration of the pure cement concrete and concrete containing QZ. However, the elevated-temperature curing at early ages does not have a negative influence on the resistance to chloride ion penetration of concrete containing BF. Comparing with curing at standard condition, the charge passed in concrete containing BF under steam curing condition decreases. The permeability of samples BF-30 and BF-45 varies from "Moderate" to "Low" and from "Low" to "Very low" at 28 days, respectively. The permeability of BF-30 also varies from "Low" to "Very low" at 90 days. From the result of TG/DTG analysis, the CH content of pure cement and composite binder containing QZ increases under high curing temperature at the later stage, while composite binder containing BF decreases. The positive effect of high curing temperature at an early stage on the pozzolanic effect of BF can compensate for the adverse effect on the resistance to chloride ion penetration at the late stage. Proper dosage can even improve resistance to chloride ion penetration of concrete.

Conclusions

(1) BF can show the pozzolanic reactivity at an early stage under room curing temperature despite low

activity. High curing temperature improves the activity of BF. The influence of high temperature on the pozzolanic reaction is greater than the influence of high temperature on cement hydration at an early stage, causing reduction in the $Ca(OH)_2$ content. However, the effect of high temperature on the pozzolanic reaction is not obvious in the later stage.

(2) The high curing temperature does not change the type of hydration product but increases the content of C–S–H gel, resulting in a significantly increased Ca–Si ratio and a slightly reduced Al–Si ratio.

(3) The high curing temperature improves the early compressive strength of the concrete containing BF and reduces later compressive strength. The positive effect of high curing temperature on the pozzolanic reaction of BF can compensate for its negative influence on resistance to chloride ion penetration. Suitable dosage of BF may improve impermeability of concrete at a high curing temperature.

Acknowledgements Authors acknowledge the support from the National Key Research and Development Program of China (2016YFC0801602).

References

1. Snellings R, Mertens G, Elsen J. Supplementary Cementitious Materials. Rev Mineral Geochem. 2012;74:211–78.
2. Damtoft JS, Lukasik J, Herfort D, Sorrentino D, Gartner EM. Sustainable development and climate change initiatives. Cem Concr Res. 2008;38:115–27.
3. Juenger MCG, Winnefeld F, Provis JL, Ideker JH. Advances in alternative cementitious binders. Cem Concr Res. 2011;41:1232–43.
4. Lothenbach B, Scrivener K, Hooton RD. Supplementary cementitious materials. Cem Concr Res. 2011;41:1244–56.
5. Liu SH, Kong YN, Wang L. A comparison of hydration properties of cement-low quality fly ash binder and cement–limestone powder binder. J Therm Anal Calorim. 2014;116:937–43.
6. Wang AQ, Zhang CZ, Sun W. Fly ash effects: II. The active effect of fly ash. Cem Concr Res. 2004;34:2057–60.
7. Yan PY, Mi GD, Wang Q. A comparison of early hydration properties of cement–steel slag binder and cement–limestone powder binder. J Therm Anal Calorim. 2014;115:193–200.
8. Gruyaert E, Robeyst N, Belie ND. Study of the hydration of Portland cement blended with blast-furnace slag by calorimetry and thermogravimetry. J Therm Anal Calorim. 2010;102:941–51.
9. Feng JJ, Liu SH, Wang ZG. Effects of ultrafine fly ash on the properties of high-strength concrete. J Therm Anal Calorim. 2015;121:1213–23.
10. Sagadin C, Luidold S, Wagner C, Wenzl C. Melting behaviour of ferronickel slags. JOM. 2016;68:3022–8.
11. Saha AK, Sarker PK. Expansion due to alkali–silica reaction of ferronickel slag fine aggregate in OPC and blended cement mortars. Constr Build Mater. 2016;123:135–42.
12. Tangahu BV, Warmadewanthi I, Saptarini D, Pudjiastuti L, Tardan MAM, Luqman A. Ferronickel slag performance from reclamation area in Pomalaa, southeast Sulawesi, Indonesia. Adv Chem Eng Sci. 2015;5:408–12.
13. Warner AEM, Díaz CM, Dalvi AD, Tarasov AV. JOM world nonferrous smelter survey, part III: nickel: laterite. JOM. 2006;58:11–20.
14. Yang T, Yao X, Zhang Z. Geopolymer prepared with high-magnesium nickel slag: characterization of properties and microstructure. Constr Build Mater. 2014;59:188–94.
15. Maragkos I, Giannopoulou IP, Panias D. Synthesis of ferronickel slag-based geopolymers. Miner Eng. 2009;22:196–203.
16. Katsiotis NS, Tsakiridis PE, Velissariou D, Katsiotis MS, Alhassan SM, Beazi M. Utilization of ferronickel slag as additive in Portland cement: a hydration leaching study. Waste Biomass Valoriz. 2015;6:177–89.
17. Rahman MA, Sarker PK, Shaikh FUA, Saha AK. Soundness and compressive strength of Portland cement blended with ground granulated ferronickel slag. Constr Build Mater. 2017;140:194–202.
18. Sekikawa S, Tsukinaga Y, Shoya M, Mechanical characteristics of high strength concrete using ferro-nickel slag fine aggregates. Summaries of technical papers of annual meeting Architectural Institute of Japan. A-1, Materials and construction. Architectural Institute of Japan (1997), pp. 23–4.
19. Choi YC, Choi S. Alkali–silica reactivity of cementitious materials using ferro-nickel slag fine aggregates produced in different cooling conditions. Constr Build Mater. 2015;99:279–87.
20. Fidancevska E, Vassilev V, Milosevski M, Parvanov S, Milosevski D, Aljihmani L. Composites based on industrial wastes III. Production of composites of Fe–Ni slag and waste glass. J Univ Chem Technol Metall. 2007;42:285–90.
21. Vassilev V, Fidancevska E, Milosevski M, Parvanov S, Milosevski D, Hristova-Vasileva T. Composites based on industrial wastes. IV. Production of porous composites from Fe–Ni slag and waste glass. J Univ Chem Technol Metall. 2007;42:369–76.
22. Zhang ZQ, Wang Q, Yang J. Hydration mechanisms of composite binders containing phosphorus slag at different temperatures. Constr Build Mater. 2017;147:720–32.
23. Han FH, Zhang ZQ, Liu JH, Yan PY. Hydration kinetics of composite binder containing fly ash at different temperatures. J Therm Anal Calorim. 2016;128:855–65.
24. Escalante-Garcıa JI, Sharp JH. The microstructure and mechanical properties of blended cements hydrated at various temperatures. Cem Concr Res. 2001;31:695–702.
25. Lothenbach B, Winnefeld F, Alder C, Wieland E, Lunk P. Effect of temperature on the pore solution, microstructure and hydration products of Portland cement pastes. Cem Concr Res. 2007;37:483–91.
26. Maltais Y, Marchand J. Influence of curing temperature on cement hydration and mechanical strength development of fly ash mortars. Cem Concr Res. 1997;27:1009–20.
27. Zhang ZQ, Zhang B, Yan PY. Hydration and microstructures of concrete containing raw or densified silica fume at different curing temperatures. Constr Build Mater. 2016;121:483–90.
28. Han FH, Wang Q, Mei YJ, Liu MT. Early hydration properties of composite binder containing limestone powder with different finenesses. J Therm Anal Calorim. 2016;123:1141–51.
29. Wang Q, Li MY, Jiang GH. The difference among the effects of high-temperature curing on the early hydration properties of different cementitious systems. J Therm Anal Calorim. 2014;118:51–8.
30. Shi MX, Wang Q, Zhou ZK. Comparison of the properties between high-volume fly ash concrete and high-volume steel slag concrete under temperature matching curing condition. Constr Build Mater. 2015;98:649–55.